Journal of Applied Electrochemistry **30**: 1361–1367, 2000.

A primary, secondary and pseudo-tertiary mathematical model of a chlor-alkali membrane cell†

P. BYRNE[1]*, P. BOSANDER[3], O. PARHAMMAR[2] and E. FONTES[3]
[1]*Faxén Laboratory, Applied Electrochemistry, Royal Institute of Technology (KTH), Teknikringen 42, SE-100 44 Stockholm, Sweden*
[2]*Permascand-Eka Chemicals R&D, PO Box 13000, SE-850 13 Sundsvall, Sweden*
[3]*Comsol AB, Tegnérgatan 23, SE-111 40 Stockholm, Sweden*
*(*author for correspondence, fax: +46 8 10 80 87, e-mail: phil@ket.kth.se)*

Received 31 July 1999; accepted in revised form 30 May 2000

Key words: chlor-alkali, current distribution, electrolysis, mass transport, model

Abstract

A theoretical study of current density and potential at the anode, membrane and cathode, of a chlor-alkali membrane cell where the electrode blades are placed vertically, is presented. A representative unit cell is modelled in primary, secondary and pseudo-tertiary current distribution models. It is shown that electrolyte and membrane resistance has the greatest effect on current distribution. Furthermore, it is shown that there is a surprisingly small influence of mass transport on current distribution, on the assumption that the diffusion layer is of constant thickness. In converse to this, it is shown that mass transport affects the anode overpotential distribution to the extent that conclusions can be made about the occurrence of side-reactions and where they occur. Finally, it is shown that it is possible to estimate tertiary behaviour with a secondary current distribution model, by using an analytic expression at the anode surface.

1. Introduction

Improvements in cell design have seen a remarkable increase in the amount of current density passing through chlor-alkali membrane cells [1]. This has led the process into areas where the feed streams are significantly close to complete ion depletion, with all the subsequent problems of concentration overpotential and side-reactions that this incurs. By creating cell geometries or conditions that are favourable to a more uniform current distribution, one is able to utilise larger portions of electrode area, and still manage localised increases in current density and therefore production. A uniform current distribution would diminish localised corrosion and ensure a more even depletion of the electrocatalyst, which undergoes wear due to gas evolution [2].

Basically, the general configuration of the chlor-alkali membrane cell allows fresh electrolyte to enter to the front of the electrodes, and bubbles to pass behind the electrodes through the gap between the electrode blades [3]. The blades can be layered horizontally, like louvres in a venetian blind [4], or vertically like slats in a fence [5]. This paper shall look at the 'lantern' cell structure found in the ICI FM-21 electrolysers, previously presented in a paper by Martin and Wragg [5]. It is generally known that the critical region of the membrane cell is the space between the membrane and electrode. Traini and Meneghini [6] reported that the membrane cell could be run with the membrane right up against the anode surface. However, this investigation will be looking at the case where there is reasonable room between the membrane and electrodes. The plan view of a horizontal cross-section of the anode, membrane and cathode is seen in Figure 1.

Primary current distribution models have previously been written to describe current density and potential distributions around the membrane cell anode [2, 5, 7, 8]. These models considered only the migratory properties of the chloride ion, whilst ignoring the convection and the complete effects of electrode kinetics. This work aims to present a model that also takes into account the kinetics of the chlorine reaction, as represented by an exponential relationship, and thus illustrate the distributions of current and potential in this secondary current distribution model. Furthermore, the article will present results from a pseudo-tertiary current distribution model, which considers the transport of chloride ions by defining a hypothetical diffusion layer. The use of an assumed diffusion layer thickness will then be investigated in the light of the work from Ibl and

† Dedicated to the memory of Daniel Simonsson

Venczel [10]. Finally, this model will be compared to an extended secondary model, which uses an analytical approximation to describe mass transport to the anode surface.

2. Problem definition

The geometry of a unit cell from the system is shown in Figure 1. It is generally assumed that the mass transport properties and conductivity in the electrolyte and membrane remain constant throughout the height of the system, and from one slat to the next. Likewise, it is assumed that potential is constant throughout all metal structures.

2.1. *Primary and secondary current distribution models*

The primary current distribution model takes into account the migratory properties of ions in the electrolyte and membrane, and does not consider diffusion mass transport or the potential that would be required to force the reactions to occur. The model is simplified by dividing the domain into three subdomains (denoted by Ω); the anolyte, membrane and catholyte. Ohm's law is assumed to adequately describe the migration of ions so that a current balance gives:

$$\nabla \cdot (-\kappa_j \nabla \phi) = 0 \quad \text{for } \Omega_{\text{all}} \tag{1}$$

where ϕ denotes potential and κ_j conductivity. The subscripts $j = 1, 2, 3$, signify the anolyte, membrane and catholyte respectively.

The boundary conditions assume potential to be constant at all of the electrodes, whilst flux through the boundaries at the top and bottom of the Figure and behind the electrodes, is assumed to be negligible. This all results in the equations:

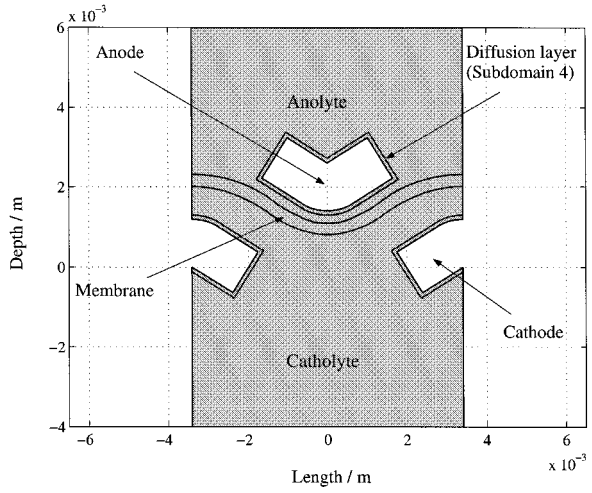

Fig. 1. Geometry of the unit cell used in the respective models. A diffusion layer has been defined for use in the pseudo-tertiary current distribution model.

$$\phi = \phi_{\text{a}} \quad \text{at } \delta\Omega_{\text{a}} \tag{2}$$

$$\phi = \phi_{\text{c}} \quad \text{at } \delta\Omega_{\text{c}} \tag{3}$$

$$-\kappa_j \nabla \phi \cdot \mathbf{n} = 0 \quad \text{at } \delta\Omega_{\text{other}} \tag{4}$$

where $\mathbf{n}$ is the unit normal vector to the respective boundaries, ϕ the potential and the subscripts 'a' denotes the anode and 'c' the cathode.

The secondary current distribution model takes into consideration anode kinetics by introducing the activation overpotential, η:

$$\eta = \phi_{\text{s}} - \phi_{\text{l}} - \Delta\phi_{\text{sl}}^{\text{eq}} \tag{5}$$

where $\Delta\phi_{\text{sl}}^{\text{eq}}$ is the equilibrium potential of the anode reaction, and the subscript 'l' denotes the electrolyte and 's' denotes the metal of the anode. Substituting this into Equation 1 gives the relative anodic overpotential:

$$\nabla \eta = -\nabla \phi_{\text{l}} \tag{6}$$

The boundary condition at the anode is described by reaction kinetics that assume that the desorption of chlorine is the rate determining step in the chlorine evolution reaction [11]

$$\kappa_j \nabla \phi \cdot \mathbf{n} = i_{\text{o}}^{\text{b}} \left\{ \exp\left(\frac{\alpha_{\text{a}} F \eta}{RT} \right) - 1 \right\} \quad \text{at } \delta\Omega_{\text{a}} \tag{7}$$

where i_{o}^{b} denotes the exchange current density, α_{a} the anodic transfer coefficient, F the faradaic constant, R the gas constant and T the temperature. The model assumes that the cathode reaction can be described reversibly, so that the boundary condition is

$$\eta = \eta_{\text{a-c}} \quad \text{at } \delta\Omega_{\text{c}} \tag{8}$$

where the term $\eta_{\text{a-c}}$ is the cathode potential relative to the anode. The other boundaries are still insulated

$$-\kappa_j \nabla \phi \cdot \mathbf{n} = 0 \quad \text{at } \delta\Omega_{\text{other}} \tag{9}$$

Table 1 provides a summary of the data used in both the primary and secondary current distribution models. The anolyte consisted of 240 g l^{-1} NaCl and the catholyte of 200 g l^{-1} NaOH at 353 K, where the respective conductivities were calculated using this data. The models are run at the comparably low current density of 3 kA m^{-2}. Membrane conductivity was obtained from Rondinini and Ferrari [12] and the kinetic data from Bard [11].

Table 1. Input data for the primary, secondary and pseudo-tertiary current distribution models

κ_1/S m^{-1}	κ_2/S m^{-1}	κ_3/S m^{-1}	i_{o}/A m^{-2}	α_{a}	T/K
50	3	100	750	29	343

2.2. *Pseudo-tertiary current distribution and the analytical mass transport limitation models*

The pseudo-tertiary current distribution model takes into consideration chloride ion transport by way of diffusion. To do this, a constant hypothetical diffusion layer around the anode is assumed. The presence of this diffusion layer adds a fourth subdomain to the system, which also includes the rather distorted assumption that chloride ion transport only occurs through diffusion, and not migration, as if it existed in a supporting electrolyte [8]. Furthermore, the mass transport of chlorine gas is not considered, which would affect the system as it takes place in the reaction kinetics at the anode, as well as providing local convection through its production [10].

Mass transport due to a concentration gradient is taken into account only in the fourth subdomain, so that the other three subdomain equations remain unchanged. Once again the production of charge does not occur in any of the domains, so that

$$\nabla \cdot (\kappa_j \nabla \phi) = 0 \quad \text{in } \Omega_j \tag{10}$$

for $j = 1, 2, 3, 4$.

As there is a further boundary between the anolyte and diffusion layer subdomains, constant concentrations are set in the first three subdomains to

$$c = c_j^{\mathrm{o}} \quad \text{in } \Omega_j \tag{11}$$

for $j = 1, 2, 3$, where c^{o} is 240 g l^{-1} (4100 mol m^{-3}), in the anolyte ($j = 1$), and set to zero in the other two subdomains. Concentration is the variable factor in the diffusion layer subdomain so that the conservation of mass yields

$$\nabla \cdot (-D_{\mathrm{l}} \nabla c) = 0 \quad \text{in } \Omega_4 \tag{12}$$

where D_{l} represents the diffusion coefficient of chloride in the diffusion layer. The kinetic expression (Equation 7) at the anode has to take into account the concentration of chloride ions at the surface, so that it can be rewritten as

$$\kappa_j \nabla \eta \cdot \mathbf{n} = i_{\mathrm{o}}^{\mathrm{b}} \left\{ \left(\frac{c^{\mathrm{s}}}{c^{\mathrm{b}}} \right)^2 \exp\left(\frac{\alpha_{\mathrm{a}} F \eta}{RT} \right) - 1 \right\} \text{ at } \delta\Omega_{\mathrm{a}} \tag{13}$$

where c^{s} is the concentration of chloride ions at the surface and c^{b} is the concentration at the reference state, which in this case is the bulk concentration. Using Faraday's law, Equation 13 can be expressed as a mass balance equation so that the boundary condition at the anode is

$$-D_{\mathrm{l}} \nabla c \cdot \mathbf{n} = -\frac{1}{F} i_{\mathrm{o}}^{\mathrm{b}} \left\{ \left(\frac{c^{\mathrm{s}}}{c^{\mathrm{b}}} \right)^2 \exp\left(\frac{\alpha_{\mathrm{a}} F \eta}{RT} \right) - 1 \right\} \text{ at } \delta\Omega_{\mathrm{a}} \tag{14}$$

The other boundary conditions are those given in the secondary current distribution model, expressed by Equations 8 and 9. The pseudo-tertiary current distribution model uses input data given in Table 1 and subsequent data presented in Table 2.

A simplified analytical model that also considers the transport of chloride ions is also investigated. The limiting current density is a way of expressing the influence that the diffusion layer thickness has on ion transport to the electrode surface. The equations for the boundary conditions are those used in the secondary current distribution model, except for that at the anode surface (Equation 7). This is found by using the following analytical expression, which is applicable for ion transport in a supporting electrolyte [14]

$$\kappa_{\mathrm{l}} \nabla \eta \cdot \mathbf{n} = \frac{i_{\mathrm{o}}^{\mathrm{b}} \left\{ \left(\frac{c}{c^{\mathrm{b}}} \right)^2 \exp\left(\frac{\alpha_{\mathrm{a}} F \eta}{RT} \right) - 1 \right\}}{1 + \frac{i_{\mathrm{o}}^{\mathrm{b}} \exp\left(\frac{\alpha_{\mathrm{a}} F \eta}{RT} \right)}{i_{\mathrm{lim}}^{\mathrm{ox}}}} \quad \text{at } \delta\Omega_{\mathrm{a}} \tag{15}$$

where $i_{\mathrm{lim}}^{\mathrm{ox}}$ is the limiting current density for the oxidation of chloride ions. The expression differs from Equation 13 in that it gives the current distribution as a function of potential and limiting current density. The models were solved using the Femlab® software package that solves partial differential equations through using the 'finite element method'.

2.3. *Gas evolution model*

The work of Ibl and Venczel [10] has led to a simple equation to describe how mass transport to an electrode surface is affected by bubble evolution. They found that the mass transport is a property of bubble evolution rate, bubble size and the mass diffusion to an electrode surface, so that

$$k_{\mathrm{l}} = 2 \left(\frac{D_{\mathrm{l}}}{\pi \tau} \right)^{1/2} \tag{16}$$

where k_{l} is the mass transport and D_{l} is diffusion of, in this case, the chloride ion to the electrode surface, and

$$\tau = \frac{2r}{3v} \tag{17}$$

where r is the radius of the bubble and v is the gas evolution rate per unit electrode area.

Table 2. Additional input data for the pseudo-tertiary current distribution model

c_1^{o}/mol m^{-3}	c_2^{o}/mol m^{-3}	c_3^{o}/mol m^{-3}	D_3/m^{-2} s^{-1}
4100	not conditioned	not conditioned	1×10^{-9}

3. Results and discussions

3.1. *Results from the primary and secondary current distribution models*

Figure 2 shows results from the primary and secondary current distribution models where overpotential is represented by the height of the diagrams, and current density by the flow-lines. The diagrams show that the major potential drop occurs through the membrane, whilst the current density distributes itself around the anode surface quite uniformly at the large free surface of the convex plane. The membrane conductivity equalises the distribution, as any localised large concentrations of current density are impossible in a medium where current conduction is poor.

The secondary model has a more uniform current distribution, as evidenced by the movement of the flow-lines towards the anode back. This occurs because the electrode kinetics curtail the current transfer process. Yet this effect is marginal and indicates that the geometry of the unit cell and the ohmic effects of the membrane and electrolytes have a far greater influence on the system than that of the electrode kinetics. This is understandable as the chlorine reaction is very fast and has a high exchange current density. Martin and Wragg basically considered the same problem and cell geometry as this paper, and derived a primary model where the overpotential was described by the product of the Tafel slope with current density [2, 5]. They discussed the use of the Butler–Volmer equation (Equation 7) at the electrode boundaries, but justified its exclusion due to the rapid kinetics prevalent at the anode, and the large industrial current densities that eventuate at lower Wagner numbers. A comparison of Figure 2 with those from Martin and Wragg [2] shows that their assumptions were reasonable.

A view of the overpotential in the secondary current distribution model is seen in the left hand diagram of Figure 3. The introduction of the reaction kinetics has

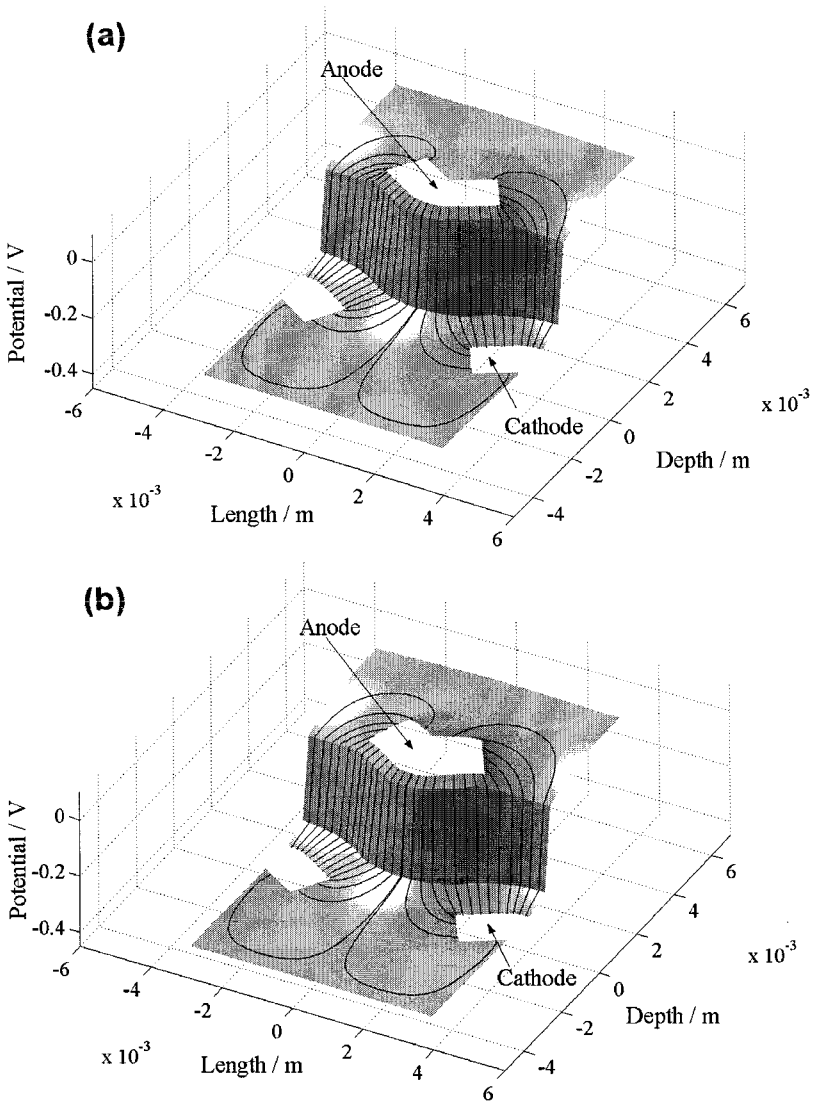

Fig. 2. Three-dimensional view of the primary (a) and secondary (b) potential distribution models in the system at the anode (top) and cathode (bottom) surfaces. The flow-lines represent current.

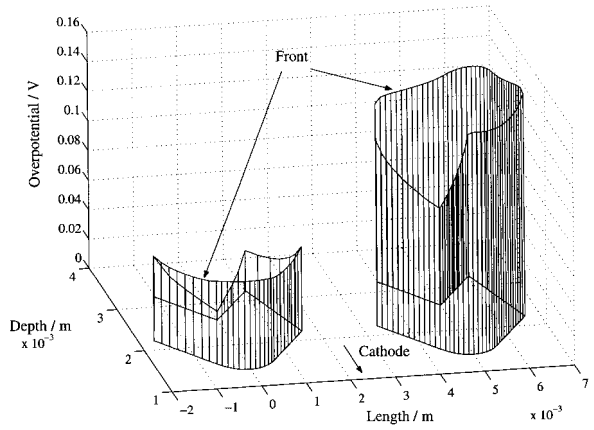

Fig. 3. Potential distribution in the solution at the anode surface for the secondary (left) and pseudo-tertiary current distribution model (right) cases.

hindered the electrode reactions to the extent that reactions had started to take place on the anode back. Current distribution in the secondary model is seen as the left diagram in Figure 4. Similar diagrams of the primary current distribution model would not show any overpotential at all, and would consist of negligible amounts of current density at the anode back.

3.2. *Results from the pseudo-tertiary current distribution model*

The right-hand diagrams in Figures 3 and 4 show the potential and current distributions from the pseudo-tertiary current distribution model. Figure 3 clearly shows that overpotential is far greater in the pseudo-tertiary model than the secondary model. Furthermore, the relative difference in potential between the anode back and front is less than in the secondary model. The pseudo-tertiary model takes into account the mass transport of chloride ions, which means that concentration overpotential is required to transport the species to the anode surface. The greater concentration overpotential has the effect of sending even more current density to the anode back, noticeable in Figure 4.

A uniform current distribution is good for the process, as it cuts down on localised catalyst destruction, anode wear and large local heat fluxes in the membrane, whilst also facilitating a greater total production rate [2]. The disadvantage with this is that overpotential increases, which gives rise to an increase in side-reactions. The most prevalent side-reaction in the chlor-alkali process, the electrochemical production of oxygen, has not been included in the model, but is a significant factor in the process. Figure 5 shows a representation of the production of chlorine and oxygen against anode potential. Shown in the Figure is the production of chlorine when diffusion does not affect ion transport (secondary model), and when it does (pseudo-tertiary model). Also shown is an exaggerated production rate of oxygen evolution. Clearly depicted in the Figure is the fact that oxygen evolution is a greater part of the total current density, when chlorine formation is affected by diffusion. In this case, the pseudo-tertiary model brings forward the conclusion that the greatest amount of side-reaction would occur at the anode front and at the corners.

A further effect that is observant in Figure 4 is the concentrations in current density occurring at the corners of the anode. As the current density is solved perpendicularly to the anode surface, it concentrates on a smaller area due to radial diffusion at the turn of the corner.

3.3. *Effect of diffusion layer thickness on the pseudo-tertiary current distribution model*

The fact that overpotential at the anode back is far lower than at the front is a possible erroneous feature of the pseudo-tertiary current distribution model. This is due to the fact that the diffusion layer thickness is

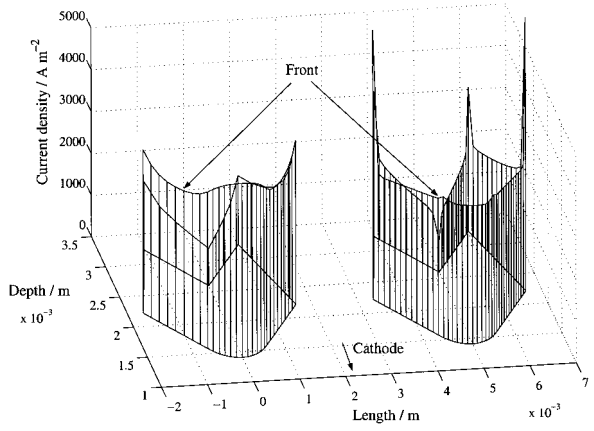

Fig. 4. Current distribution at the anode (perpendicular to the surface) for the secondary (left) and pseudo-tertiary (right) current distribution model cases.

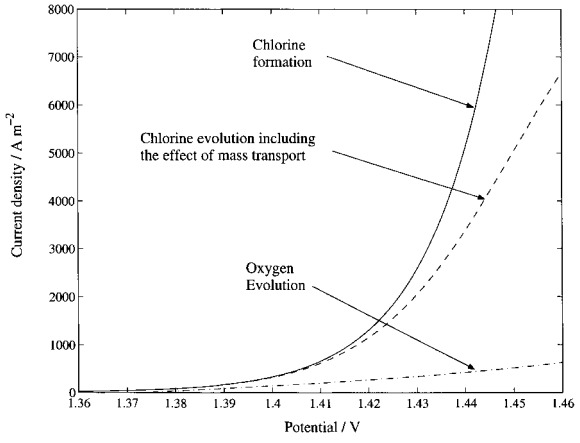

Fig. 5. Schematic illustration of the production rate of chlorine and oxygen (exaggerated to about 150 times – chain line) against anode potential. Chlorine production rate is shown when the effect of mass transport limitations is considered (dashed line) and not considered (solid line).

assumed as being constant, which results in a failure to consider the real convective properties of the system and the effect that gas evolution would have on ionic transport close to the anode. The overall macro-convection of the system is governed by the buoyant rise of chlorine bubbles. An increase in bubble production brings about an increase in convection and a decrease in diffusion layer thickness. Therefore, as production is greater on the anode front, the macro- and micro-convective effects would favour this region. This would mean that there would be an average diffusion layer that is thinner at the front than at the back. The equilibrium situation is a stand-off between the positive effects of the bubbles and the negative effects of increased electrolyte resistance, due to the bubbles, and a diminished concentration of chloride ions.

The micro- and macro-convective properties of growing and moving bubbles are described in Vogt's summary of gas evolving electrodes [9]. Using the equations of Ibl and Venczel [10] (Equations 16 and 17) and substituting in an average chlorine bubble diameter of 200 μm, a number of current densities and the corresponding diffusion layer thicknesses were calculated (see Table 3).

Figure 6 shows the current distribution from the case when the diffusion layer thickness is 50 μm, as the diagram on the right, and compares it to the previous case where the thickness has been set at 100 μm. Figure 7 also shows the cases from when the diffusion layer thickness was set to 16.2 μm (left) and 8.2 μm (right). These figures show that a decrease in diffusion layer thickness does not bring about radical changes in the current distribution. The shapes of the graphs and values of current density differ only marginally between the four cases.

Figure 8 shows, instead, that the effect of diffusion layer thickness on the distribution of anode overpotential is significant. The Figure shows a greater overpotential from the case where diffusion layer thickness was set to 100 μm (left) and than when it was 50 μm (right). The relative difference between the overpotential at the front and back is greater the thicker the diffusion layer is. If one were to assume that there was a diffusion layer thickness of 100 μm at the back, and only 8.2 μm at the front, the model would show overpotential being more-or-less equal around the anode.

First, it can be concluded that the pseudo-tertiary current distribution model, that only considers the transport of chloride ions and assumes a constant diffusion layer thickness, is reasonable for modelling current distributions. Yet, due to the fact that overpotential is sensitive to diffusion layer thickness and reality indicates that this thickness varies around the anode, it can be concluded that the model is not so applicable for predicting potential distributions and possible areas of side-reaction occurrence.

Table 3. Diffusion layer thickness, calculated from Equations 16 and 17, taken from the model of Ibl and Venczel [10]

i_T/A m^{-2}	135	1350	5000
δ/μm	50	16.2	8.2

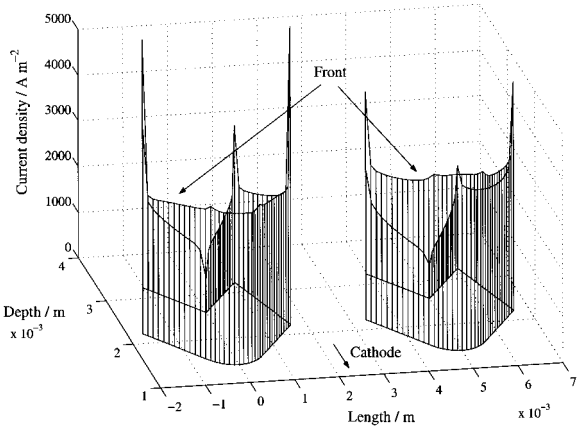

Fig. 6. Current distribution at the anode (perpendicular to the surface) for the pseudo-tertiary current distribution model, where the diffusion layer thickness is set to 100 μm (left) and 50 μm (right).

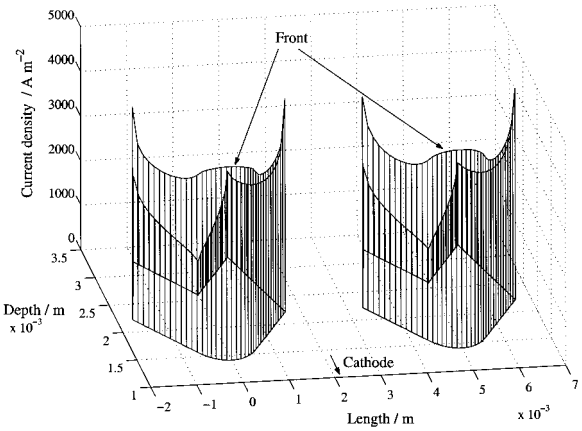

Fig. 7. Current distribution at the anode (perpendicular to the surface) for the pseudo-tertiary current distribution model, where the diffusion layer thickness is set to 16.2 μm (left) and 8.2 μm (right).

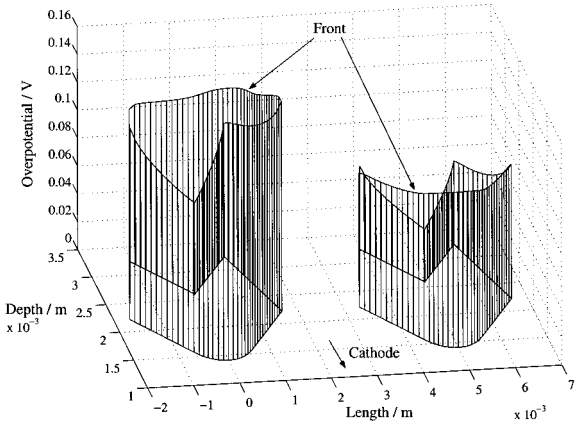

Fig. 8. Potential distribution at the anode for the pseudo-tertiary current distribution model, where the diffusion layer thickness is set to 100 μm (left) and 50 μm (right).

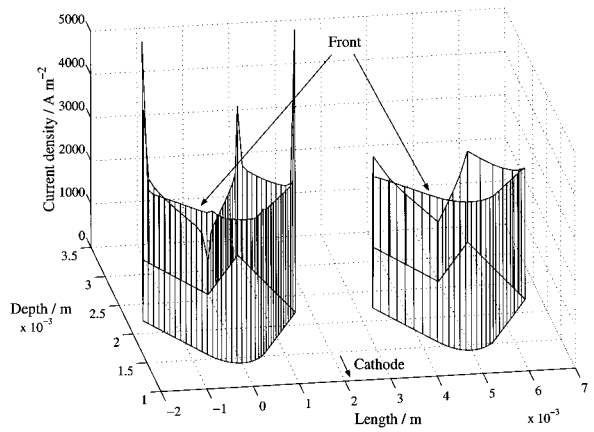

Fig. 9. Current distribution at the anode (perpendicular to the surface) for the pseudo-tertiary current distribution model (left) and the analytical mass transport limitation model (right), where the diffusion layer thickness is set to 100 μm and the concentration bulk is 4100 mol m^{-3}.

3.4. *Comparison between pseudo-tertiary current distribution and analytical mass transport limitation models*

The pseudo-tertiary current distribution model uses a diffusion layer thickness, which must be laboriously defined in the computational language, whereas the mass transport limitation analytical model uses a variable; i_{lim} (Equation 15). This model uses a value for i_{lim} that corresponds to the bulk concentration (4100 m^3 mol^{-1}) and diffusion layer thickness applied above (100 μm). It is a lot easier to express i_{lim} as a function of position and current rather than it is to change the geometry system every time a different case is to be investigated. Figure 9 shows the current distributions from both models are similar and, although not shown here, the same is the case when comparing the potential distributions. The analytical model is quite decent as an initial indication of current distribution, but relies heavily on the assumption that there is a supporting electrolyte. This assumption implies that chloride depletion has no impact on electrolyte conductivity, which is basically not true. The pseudo-tertiary current distribution model has the potential to be further developed to include this and a number of other assumed properties.

References

1. T. Borucinski and K. Schneiders, 'A new generation of the Krupp Uhde single-element design', *Mod. Chlor-Alkali Technol.* Vol. 7 (Ellis Horwood, Chichester, UK, 1998) 105–112.
2. A.D. Martin, A.A. Wragg and J.C.R. Turner, 'Numerical modelling of membrane cell primary current and potential distributions. Part 1: Finite difference approach and effect of electrode shape', *IChemE Symposium Series No. 98*, (1986), p. 35.
3. K. Borucinski and K. Schneiders, *op. cit.* [1], chapter 13. (Ellis Horwood, 1996).
4. G. Bergner, 'Operating experience gained with the bipolar Hoescht–Udhe membrane cell', *Mod. Chlor-Alkali Technol.* Vol. 3, (Ellis Horwood, Chichester, UK, 1986), chapter 13.
5. A.D. Martin and A.A. Wragg, 'Numerical modelling of membrane cell primary current and potential distributions. Part 2: Membrane position, electrode position and electrolyte effects', 4th European symposium on 'Electrochemical Engineering', Prague, Czech Republic (1996).
6. C. Traini and G. Meneghini, 'Improvement of electrode performance from combined optimization of coating composition and structural design', *Mod. Chlor-Alkali Technol.* **5** (1992) 269–280.
7. J.T. Keating, 'Sulphate deposition and current distribution in membranes for chlor-alkali cells', Proceedings from the symposium on 'Electrochemical Engineering in the Chlor-Alkali and Chlorate Industries', Electrochemical Society, (1988).
8. J.S. Newman, 'Electrochemical Systems', 2nd edn (Prentice-Hall, Englewood Cliffs, NJ, 1991).
9. H. Vogt, 'Comprehensive Treatise of Electrochemistry', Vol. 6 (1983a), p. 445.
10. N. Ibl and J. Venczel, *Met. Oberfläche* **24** (1970) 1105.
11. J. Bard, 'Encyclopaedia of Electrochemistry of the Elements', Vol. 1 (Marcel Dekker, New York, 1973).
12. S. Rondinini and M. Ferrari, 'Resistivity behaviour of perfluorinated ionic membranes in the chlor-alkali electrolytic process', Proceedings Electrochemical Society (1986), volume 86–13.
13. N. Ibl, E. Adams, J. Venczel and E. Schalch, *Chem. Ing. Tech.* **43** (1971) 202–215.
14. D. Simonsson and G. Lindbergh, 'Elektrokemi och korrosion', Applied Electrochemistry, Royal Institute of Technology, Stockholm (1997).